The Plant Cell, Vol. 20: 2146–2159, August 2008, www.plantcell.org

Arabidopsis TONNEAU1 Proteins Are Essential for Preprophase Band Formation and Interact with Centrin [W]

Juliette Azimzadeh,[a,1,2] Philippe Nacry,[a,1,3] Anna Christodoulidou,[a,1,4] Stéphanie Drevensek,[a,1] Christine Camilleri,[a] Nardjis Amiour,[a] François Parcy,[b] Martine Pastuglia,[a] and David Bouchez[a,5]

[a] Institut Jean-Pierre Bourgin, Station de Génétique et d'Amélioration des Plantes UR254, Institut National de la Recherche Agronomique, Centre de Versailles, F-78000 Versailles, France

[b] Laboratoire de Physiologie Cellulaire Végétale, Centre National de la Recherche Scientifique/Commissariat à l'Energie Atomique/Institut National de la Recherche Agronomique/Université Joseph Fourier, 38054 Grenoble Cedex 9, France

Plant cells have specific microtubule structures involved in cell division and elongation. The *tonneau1* (*ton1*) mutant of *Arabidopsis thaliana* displays drastic defects in morphogenesis, positioning of division planes, and cellular organization. These are primarily caused by dysfunction of the cortical cytoskeleton and absence of the preprophase band of microtubules. Characterization of the *ton1* insertional mutant reveals complex chromosomal rearrangements leading to simultaneous disruption of two highly similar genes in tandem, *TON1a* and *TON1b*. TON1 proteins are conserved in land plants and share sequence motifs with human centrosomal proteins. The TON1 protein associates with soluble and microsomal fractions of *Arabidopsis* cells, and a green fluorescent protein–TON1 fusion labels cortical cytoskeletal structures, including the preprophase band and the interphase cortical array. A yeast two-hybrid screen identified *Arabidopsis* centrin as a potential TON1 partner. This interaction was confirmed both in vitro and in plant cells. The similarity of TON1 with centrosomal proteins and its interaction with centrin, another key component of microtubule organizing centers, suggests that functions involved in the organization of microtubule arrays by the centrosome were conserved across the evolutionary divergence between plants and animals.

INTRODUCTION

Because the cell wall constrains cell division, limits cell elongation, and prevents cell migration, land plants have evolved specific cellular structures that are central to processes of cell division and elongation. In particular, the plant microtubule (MT) cytoskeleton assembles into several spatially independent arrays, some unique to plant cells, which form at different times during the cell cycle and cell differentiation (Wasteneys, 2002). Unlike other eukaryotes, cells of land plants lack a conspicuous MT organizing center like a centrosome except, briefly, during formation of flagellate sperm cells of nonsiphonogamous plants (Pastuglia and Bouchez, 2007). Consequently, organization of MTs into highly structured networks is not as tightly coupled to the nucleation process as it is in cells possessing a centrosome, where, in addition to nucleation per se, capping and anchoring activities also participate in organizing a radial MT network (Dammermann et al., 2003). By contrast, nucleation sites of plant cells are located on the nuclear surface (Stoppin et al., 1994) or dispersed at the cell cortex (Shaw et al., 2003) in connection with extant MTs (Murata et al., 2005). In addition to temporal and spatial positioning of nucleation sites and control of their activity, establishment and maintenance of cortical arrays likely involves other activities like anchoring, severing, treadmilling, bundling, and control of the dynamic properties of MTs through selective stabilization (Dixit and Cyr, 2004; Lloyd and Chan, 2004). However, there is still much to learn about molecular mechanisms that control the dynamics of plant MTs, anchor them to membranes, drive the formation of cortical arrays, and link the cytoskeleton to the cell cycle and the cell wall (Van Damme et al., 2007).

The preprophase band (PPB), a transient ring of cortical MTs specific to plant cells, precisely delineates the location of the division plane at the onset of mitosis (Mineyuki, 1999). The PPB is a shared, derived character of land plants, not present in their charophycean green algae ancestors (Graham, 1996). This conspicuous ring of MTs is formed in most vegetative cells of land plants with very few exceptions, like cœnocytes or filamentous moss protonemata. It is also absent in meiotic divisions and subsequent generative divisions during gametogenesis. Concomitant with PPB disappearance and breakdown of the nuclear envelope, the mitotic spindle is formed in an acentriolar fashion.

[1] These authors contributed equally to this work.

[2] Current address: Department of Biochemistry and Biophysics, University of California, San Francisco, CA 94143-2200.

[3] Current address: Laboratoire de Biochimie et Physiologie Moléculaire des Plantes, Institut National de la Recherche Agronomique/Centre National de la Recherche Scientifique/Agro-M/UM II, 34060 Montpellier, France.

[4] Current address: European Food Safety Authority–Genetically Modified Organisms Unit, DUS/A/00.10, 43100 Parma, Italy.

[5] Address correspondence to bouchez@versailles.inra.fr.

The author responsible for distribution of materials integral to the findings presented in this article in accordance with the policy described in the Instructions for Authors (www.plantcell.org) is: Martine Pastuglia (pastuglia@versailles.inra.fr).

[W] Online version contains Web-only data.

www.plantcell.org/cgi/doi/10.1105/tpc.107.056812

At the end of mitosis, another plant-specific cytoskeletal structure, the phragmoplast, drives the formation of the new cell plate. It assembles between daughter nuclei and grows centrifugally toward the cell cortex, eventually reaching the cortical site previously marked by the PPB. Numerous studies suggest a key role of the PPB in the determination of the division plane in plant cells (Mineyuki, 1999), but its precise role remains unclear, and the nature of the information deposited at the cell cortex, maintained during mitosis, and recognized during cytokinesis and phragmoplast growth is unknown, although several proteins potentially involved in such processes are being identified (Buschmann et al., 2006; Van Damme et al., 2006, 2007; Walker et al., 2007).

Very few mutations specifically affect PPB formation. The TANGLED gene of maize (*Zea mays*) is required for spatial guidance of expanding phragmoplasts, and the *tangled* mutation affects the position of both PPBs and phragmoplasts in leaf epidermal maize cells (Cleary and Smith, 1998). In the *Arabidopsis thaliana microtubule organization1-1* mutant, one-half of dividing cells fail to form PPBs prior to spindle formation, and when PPBs form, some of them are aberrant (Kawamura et al., 2006). The *Arabidopsis tonneau1* (*ton*1) and *fass/tonneau2* mutants are the only plant mutants specifically unable to form a PPB, which correlates with abnormal positioning of the cell plate in mutant cells (Traas et al., 1995; Camilleri et al., 2002). The *fass* gene was previously shown to encode a phosphatase 2A regulatory subunit (Camilleri et al., 2002). Consistent with a role of FASS in determination of the division plane at the onset of mitosis, it has been shown recently that FASS/TON2 is required for proper localization of TANGLED–yellow fluorescent protein (YFP) at the cortical division site throughout mitosis and cytokinesis (Walker et al., 2007).

In this study, we report on the characterization of the TON1 genes and proteins. Interestingly, several lines of evidence point to an evolutionary link between the TON1 proteins, the organization of the plant cell cortical cytoskeleton, and centrosome functions in animal cells.

RESULTS

PPB Formation Is Not Required for Entry into Mitosis

The *ton1* mutant was obtained by T-DNA insertional mutagenesis (Traas et al., 1995). The shape and cellular organization of the plants are extremely modified, although general body pattern and relative positions of organs are not altered (Figures 1A to 1H). The *ton1* mutant is indistinguishable from a *fass* loss-of-function allele (Figure 1I). We analyzed MT organization in *ton1* cells using either tubulin immunolabeling or expression of a green fluorescent protein–microtubule binding domain (GFP-MBD) MT marker; both techniques gave similar results. As already noted (Traas et al., 1995), mutant plants displayed strong alterations in the organization of cells (Figures 2I and 2J) and of the cortical MT interphase array (Figures 2A to 2H); in comparison with the wild type, the proportions of hypocotyl cells showing transverse, longitudinal, or mixed orientation of the cortical interphase array were strongly distorted in the mutant (Figures 2A and 2B, Table

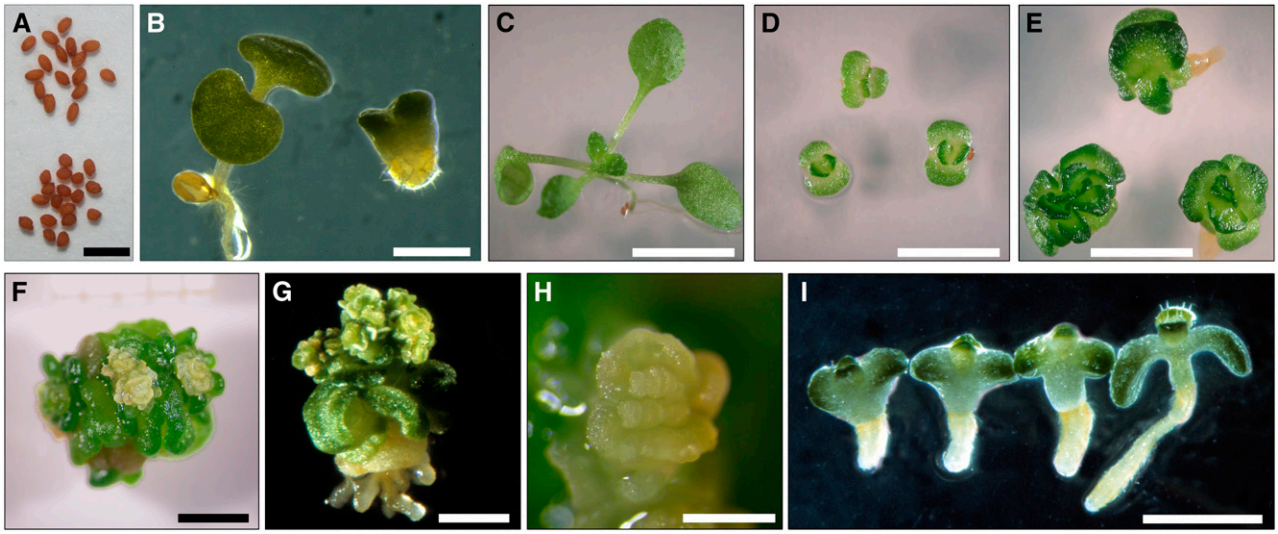

Figure 1. Developmental Phenotype of the *ton1* Mutant.

(A) *ton1* mutant seeds (bottom) have a modified shape compared with the wild type (top). Bar = 1 mm.
(B) In vitro–grown wild-type (left) and *ton1* mutant plantlets 7 d after germination. Bar = 5 mm.
(C) to **(E)** Wild-type plant **(C)** and *ton1* mutants 11 d **(D)** and 3 weeks **(E)** after germination. Bars = 5 mm.
(F) and **(G)** *ton1* mutant plant 6 weeks after germination. Bars = 5 mm.
(H) Close-up on a *ton1* mutant flower. Bar = 1 mm.
(I) From left to right: in vitro–grown *ton1*, *fass*2, *fass*11, and *fass*12 (= *ton*2-12; Camilleri et al., 2002) mutants 10 d after germination. *ton1* and *fass*2 are in the Wassilewskija (Ws) background, while *fass*11 and 12 are in the Landsberg *erecta* (L*er*) background. Bar = 5 mm.

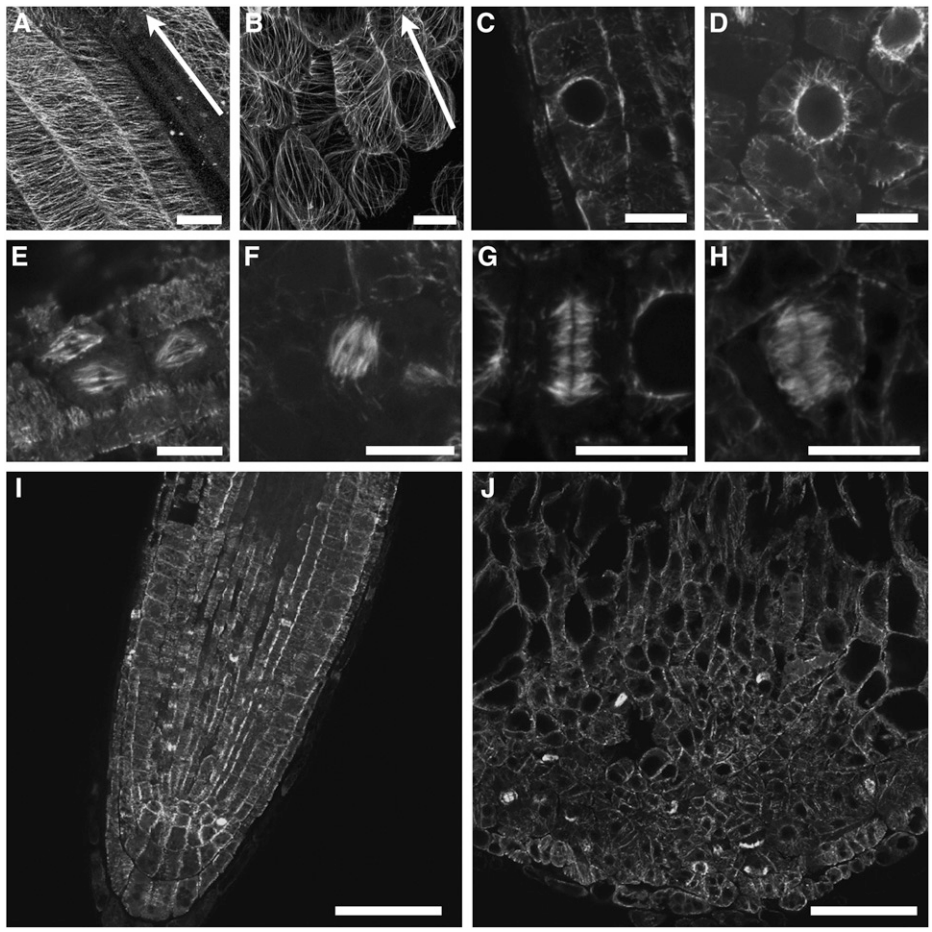

Figure 2. MT Organization in the *ton1* Mutant.

(A) and **(B)** Interphase cortical arrays of MTs in wild-type **(A)** and *ton1* **(B)** hypocotyl cells of transgenic *Arabidopsis* expressing GFP-MBD, which labels MTs. Arrows indicate the direction of the long axis of hypocotyls.
(C) to **(J)** Immunolocalization in root cells using an anti-α-tubulin antibody.
(C) A typical wild-type PPB of MTs just before transition toward spindle assembly.
(D) Preprophase nuclei in dividing *ton1* mutant cells, showing dense accumulation of MTs around the nuclei and no evidence of cortical structures.
(E) Wild-type spindles.
(F) A *ton1* mutant spindle.
(G) Wild-type phragmoplast.
(H) *ton1* mutant phragmoplast.
(I) A wild-type *Arabidopsis* root tip.
(J) A *ton1* mutant root tip, showing alteration in cell shape, size, number, and loss of global cellular organization.
Bars = 50 μm in **(A)**, **(B)**, **(I)**, and **(J)** and 10 μm in **(C)** to **(H)**.

1). More than 58% of mutant cells exhibited an absence of preferential orientation compared with 8% in wild-type cells. The *ton1* mutant was originally described as being devoid of detectable PPB or MT accumulation at the cortex in dividing cells (Traas et al., 1995). Our analyses using either tubulin immunostaining or expression of the GFP-MBD marker confirm the complete absence of PPB formation in *ton1* mutant cells for every developmental stage and organ examined. Instead, as already noted for *fass* mutants (McClinton and Sung, 1997; Camilleri et al., 2002), a strong accumulation of perinuclear MTs occurs in premitotic *ton1* mutant cells (Figure 2D) at a density never observed in wild-type cells (Figure 2C). Frequencies of MT patterns in root tip cells were compared between wild-type and mutant plants: the distribution of interphase, preprophase, spindle, and phragmoplast stages was highly similar between the wild type and the mutant (Table 2). This showed that the *ton1* mutation does not notably impair the timing of cell division and that *ton1* cells can overcome the absence of PPB formation and proceed into mitosis. After preprophase, typical mitotic spindles are observed in mutant cells (Figures 2E and 2F) as well as phragmoplasts during late anaphase (Figures 2G and 2H), showing that functional TON1 proteins are not required for the formation of mitotic arrays.

Table 1. Preferential Orientation of Cortical MT Arrays in Wild-Type and Mutant Root Tip Cells

Orientation	Wild Type	*ton1*
Transverse	62.7%	21.9%
Longitudinal	29.3%	19.9%
NP	8.0%	58.2%
Total cells	225	306

The preferential orientation of the cortical interphase MT array was analyzed in hypocotyls of wild-type (five plants, 225 cells) and *ton1* (four plants, 306 cells) 6-d-old plants expressing the GFP-MBD marker, taking the hypocotyl axis as a reference. The entire length of wild-type and *ton1* hypocotyls was scored. Distributions are strongly dissimilar ($\chi^2 = 148$, $P < 0.001$). NP, no preferential orientation.

Altogether, these data show that TON1 proteins are essential for the organization of cortical MT arrays during interphase and preprophase. During mitosis, the absence of TON1 does not notably impair formation and function of the mitotic spindle and phragmoplast, although slight alterations in phragmoplast morphology can be observed in mutant cells (data not shown) that could be the result of altered phragmoplast guidance linked to the absence of PPB.

The TON1 Locus Contains Two Highly Similar Genes in Tandem

Genetic analysis of the T-DNA insertion line ACL4 revealed complex chromosomal rearrangements, including a reciprocal translocation and a pericentric inversion (Nacry et al., 1998) (details in Supplemental Figure 1 online). Genetic and physical mapping showed that the *ton1* mutation results from disruption of a locus located at a translocation breakpoint on chromosome 3. This region contains two nearly identical genes in tandem orientation that were named *TON1a* and *TON1b*. Comparison of wild-type and mutant genomic sequences revealed a 1.4-kb deletion in ACL4, affecting both *TON1* genes (Figure 3).

To formally establish that the *ton1* phenotype is caused by simultaneous disruption of the *TON1a* and *b* genes, we performed complementation analysis of the *ton1* mutant. Constructs harboring either the full *TON1a+TON1b* genomic region, the *TON1a* gene alone, or the TON1b cDNA under the control of the 35S promoter were all able to complement the mutant phenotype (see Supplemental Figure 2 online). Silencing of the P35S-TON1b construct in a *ton1* mutant background led to a range of phenotypic complementation from almost mutant to wild-type (see Supplemental Figure 2 online).

RT-PCR experiments (Figure 4) and analysis of available microarray data (Menges et al., 2003; Zimmermann et al., 2004) (see Supplemental Figure 3 online) showed that *TON1a* and *b* genes have similar constitutive expression patterns, showing little variation during development, during the cell cycle, or in response to a series of biotic and abiotic stresses.

Taken together, these data demonstrate that we have isolated the locus responsible for the *ton1* phenotype and indicate that, consistent with their high sequence identity and similar expression pattern, the functions of the two *TON1* genes are fully redundant.

In contrast with the loss-of-function *ton1* mutant, transgenic *Arabidopsis* lines overexpressing either TON1a or TON1b cDNA driven by the 35S promoter did not show any growth and development defect in standard growing conditions (see Supplemental Figure 2 online).

TON1 Proteins Are Strongly Conserved in Land Plants and Share Conserved Sequence Motifs with Human Centrosomal Proteins

TON1a and *TON1b* genes encode predicted polypeptides of 29 kD and share ~85% amino acid identity. TON1 ESTs from angiosperms and gymnosperms were also identified in databases, all displaying high sequence identity to TON1a and b along their entire length. In addition, a moss *Physcomitrella patens* EST sequence, corresponding to the first 114 amino acids, also shows strong similarity with *Arabidopsis* TON1a and b (63% identity) (Figure 5A). Database searches also identified several partially similar proteins, originating from a variety of nongreen species from protists to vertebrates (Figures 5B). The N-terminal region of TON1a and b is similar to the N-terminal region of two human proteins: FOP (for FGFR1 Oncogene Partner) (Popovici et al., 1999) and OFD1 (for Oral Facial Digital 1) (Ferrante et al., 2001) (Figure 5A). Interestingly, FOP and OFD1 both localize to the centrosome in human cells (Andersen et al., 2003; Romio et al., 2003; Yan et al., 2006). Multiple alignment and motif analysis of these proteins revealed three regions of strong sequence conservation: a previously unidentified motif of 33 residues at the N terminus (TOF motif, for TON1, OFD1, and FOP); a 34-residue LisH dimerization motif (Emes and Ponting, 2001); and a region with a conserved PLL triad that, according to structural data (Mikolajka et al., 2006), is expected to participate in LisH-mediated dimerization (Figure 5A). TON1 and FOP N termini display a similar organization, including a phosphorylation site situated next to the PLL motif (Benschop et al., 2007; Sugiyama et al., 2008) and a short Ser-rich region (Figure 5C).

TON1 is not found in sequences of green algae currently available, and the *Chlamydomonas* FOP protein (Figure 5B) is equally distant to FOP and to land plant TON1s. The occurrence of typical TON1 proteins seems therefore evolutionary correlated

Table 2. Frequency of MTs Patterns in Wild-Type and Mutant Root Tip Cells

Stage	Wild Type	*ton1*
Interphase	91.8%	92.7%
Preprophase	3.9%	3.7%
Spindle	1.1%	0.6%
Phragmoplast	3.3%	3%
Total cells	1219	1552

Tubulin immunostaining of root tips as shown in Figures 2I and 2J allowed comparison of MT patterns between the wild type and mutant. Four roots/1552 cells and five roots/1219 cells were scored for the mutant and the wild type, respectively. Preprophase stage was determined by occurrence of a PPB in the wild type (Figure 1C) and by perinuclear accumulation of MTs in the mutant (Figure 1D). Distributions of stages are highly similar ($\chi^2 = 1.81$, $P = 0.61$).

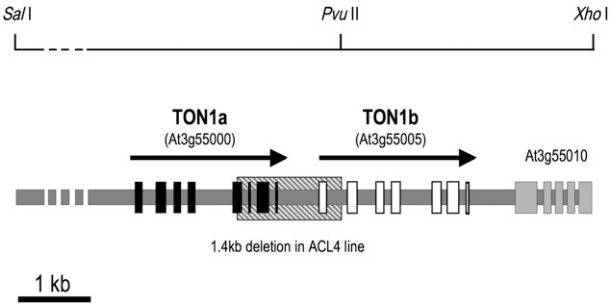

Figure 3. Structure of the TON1 Locus.

The *TON1a* gene contains eight exons (black boxes), whereas the *TON1b* gene has only seven exons (white boxes), as *TON1*a exons 6 and 7 are fused in *TON1b*. The 1.4-kb deletion found at the translocation breakpoint in the ACL4 line is boxed. Restriction sites corresponding to fragments used in complementation experiments are shown on top; their positions on Arabidopsis Genome Initiative pseudomolecules (version 5, ftp://ftp.Arabidopsis.org/home/tair/Sequences/) are: SalI 20,387,939 bp; PvuII 20,395,408; XhoI 20,398,868 bp.

with the acquisition of the PPB in embryophytes. When genomic sequences are available, the position of the first intron is strictly conserved among plant and animal TOF-containing proteins, further demonstrating a common evolutionary origin (see Supplemental Figure 4 online).

A TON1 Pool Associates with Membranes

To address the subcellular localization of TON1, we raised an antibody against full-length TON1b protein produced in *Escherichia coli*. In a protein gel blot of total proteins, the anti-TON1 antiserum labeled a protein band at the expected size of ~30 kD, which is undetectable in *ton1* mutant extracts (Figure 6). TON1 proteins were found both in the soluble and microsomal fractions from plant tissues. TON1 was released from microsomes after exposure of the pellet to basic pH (Figure 6) or mild detergents (data not shown), indicating extrinsic association with membranes. These results are consistent with recent proteomics results where both TON1a and TON1b were detected in a highly purified cortical fraction (i.e., proteins associated with the cytosolic face of the plasma membrane) (Benschop et al., 2007). In our experiments, TON1 closely follows the pattern of tubulin (Figure 6), which is known to fractionate into a soluble and a membrane-associated pool. Since TON1 does not contain any potential membrane-spanning or anchoring domain, this association to membranes is likely to be indirect and mediated by TON1 partners at the cell's cortex.

TON1 Labels the PPB and the Interphase Cortical MT Array

To further assess TON1 subcellular localization, we generated GFP-TON1a fusions driven either by the 35S promoter or by the native TON1a promoter. Stable transgenic *Arabidopsis* lines were obtained both in a wild-type Ws and in a *ton1* mutant background. Both constructs were able to partially rescue the phenotype in a mutant background, showing that the GFP-TON1a fusion protein is at least partially properly localized and active (data not shown). In both backgrounds, expression of GFP fusions varied between lines and between cells in a particular line, suggesting partial instability and/or silencing of the fusion proteins. However, among lines exhibiting GFP fluorescence, P35S- and PTON1a-driven constructs weakly but consistently labeled structures at the cell cortex, in addition to a general diffuse cytoplasmic fluorescence. In the division zone of the root tip, the GFP-TON1a fusion was observed in PPB-like rings, in cells presumably corresponding to those at the preprophase stage (Figures 7A and 7B; see confocal series in Supplemental Figure 5 online). Labeling of spindle or phragmoplast was not observed, indicating that TON1a is not present on these mitotic structures. In addition to GFP-TON1a association with PPB in the division zone of the root, labeling of transverse cell ends was also frequently observed (Figure 7A).

To confirm GFP-TON1a localization at the PPB, transformed tobacco (*Nicotiana tabacum*) roots expressing the GFP-TON1a fusion under the control of the 35S promoter were obtained. Two clones exhibiting GFP expression were selected and analyzed by confocal microscopy. GFP fluorescence in these two clones displayed a localization similar to the *Arabidopsis* lines expressing the same fusion. Both PPB (Figure 7D) and cross-walls (Figure 7C) were consistently labeled.

The GFP-TON1a marker was further studied in *Arabidopsis* expanding hypocotyl cells. In these interphase cells, the GFP-TON1a labeling appeared as a punctate and faint staining along

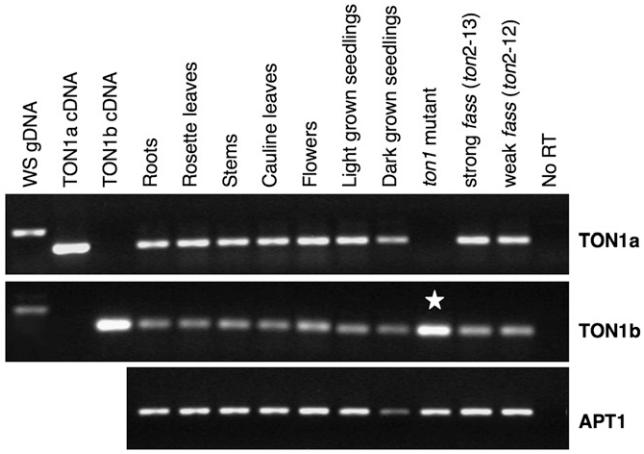

Figure 4. Analysis of TON1a and TON1b Gene Expression by RT-PCR.

RT-PCR analyses were performed as described (Camilleri et al., 2002) using gene-specific primers: a 461-bp RT-PCR fragment was obtained for the TON1a transcript using the primers Spec1aF and Spec1aR, specific for the TON1a gene, and a 281-bp RT-PCR fragment was obtained for TON1b using the primers Spec1bF and Spec1bR, specific for the TON1b gene. The constitutively expressed *APT1* gene (Moffatt et al., 1994) was used as a control (564-bp RT-PCR fragment with primers APT-RT1 and APT-RT2). WS gDNA, Ws genomic DNA; No RT, negative control (no reverse transcriptase). In the *ton1* mutant, primers specific for the TON1b gene detect a fusion transcript (asterisks) between (1) the Basta resistance gene present in the T-DNA used for insertion mutagenesis and (2) the 3′ end of the TON1b gene.

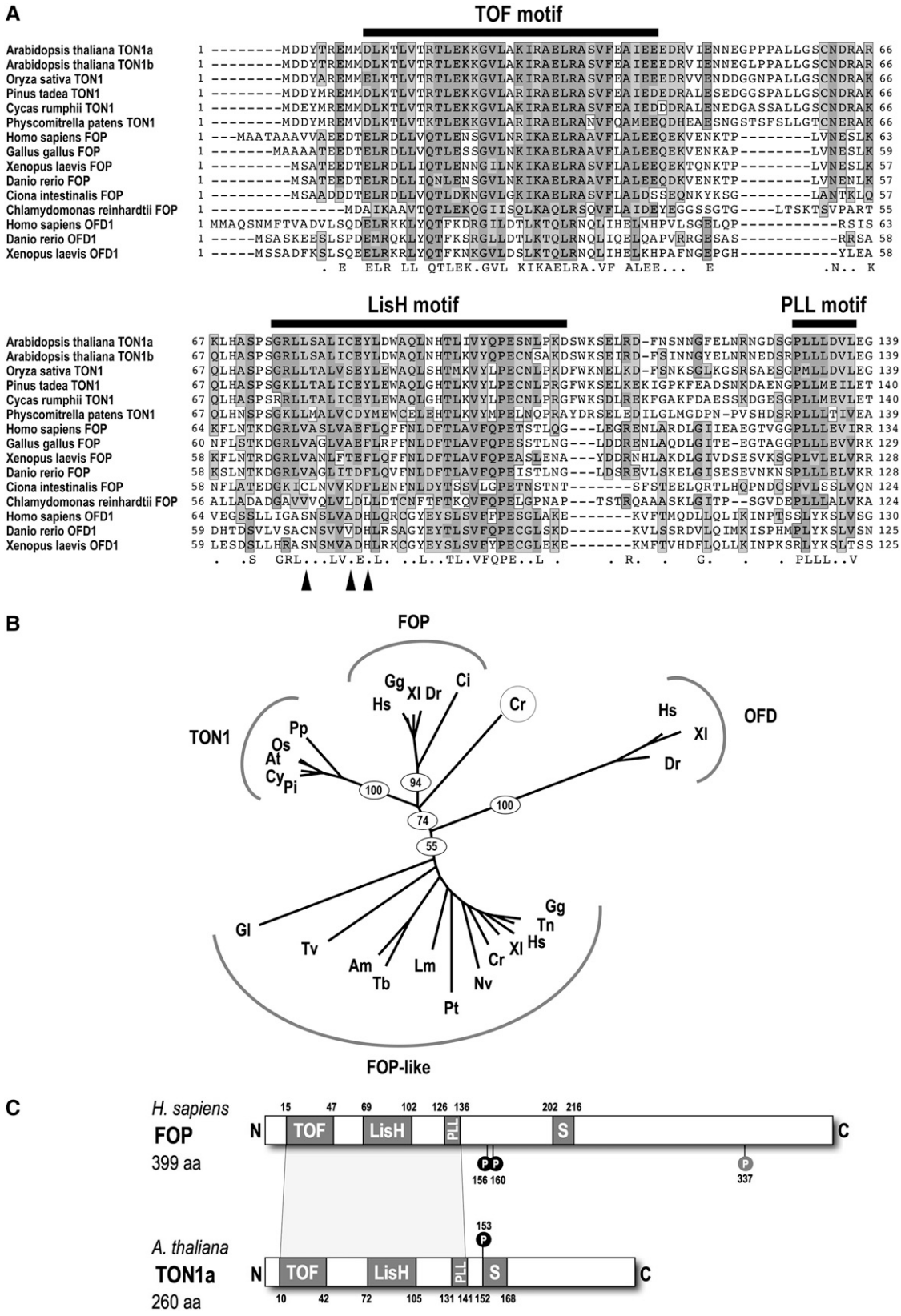

Figure 5. Multiple Alignment of Proteins Related to TON1 Defines a New Conserved Protein Motif.

dense linear arrays mostly organized transversally to the cell elongation axis. These arrays strongly resemble typical interphase cortical arrays of MTs in elongating cells (Figures 7E and 7F). To confirm association of GFP-TON1a with MTs, we treated hypocotyls cells expressing GFP-TON1a with the MT depolymerizing drug oryzalin. Oryzalin at 10 μM induced fragmentation and disappearance of GFP-TON1a cortical labeling starting at 5 min after treatment, confirming dependence of TON1a localization upon MTs (Figures 7G to 7J). Therefore, TON1's peripheral association to the membrane (Figure 6) likely reflects its recruitment to cortical MTs. The acidic nature of TON1a and b and absence of potential domain involved in MT binding suggest that other partners are required for this targeting.

Altogether, fractionation experiments, published proteomics results, and our GFP labeling studies in *Arabidopsis* and tobacco give a consistent view of TON1's subcellular localization: TON1a and b proteins are present as both a cytoplasmic pool and a cortex-associated pool, where they are able to associate with different cortical cytoskeletal structures, the PPB and interphase MT arrays.

TON1 Interacts with Centrin, a Major Component of Eukaryotic MT Organizing Centers

To identify TON1 protein partners, the full-length TON1b protein was used as a bait in a two-hybrid interaction screen in yeast using an *Arabidopsis* cDNA library from young siliques (Grebe et al., 2000). From 250 positive clones analyzed, 26 clones originated from the same gene (At3g50360), corresponding to four independent cDNAs of different sizes. At3g50360 encodes CEN1, a protein highly similar to centrins (80% similarity to *Chlamydomonas* centrin). Centrins are EF-hand calcium binding proteins closely related to calmodulin. They are essential components of MT organizing centers in a wide range of organisms from protists, fungi, and animals to green algae and lower plants and make contractile fibers connecting centrioles/basal bodies and other centrosomal elements (Salisbury, 1995). We tested the ability of the other *Arabidopsis* centrin isoform, CEN2 (65% identical to CEN1), to interact with TON1b in yeast; no significant interaction between TON1b and CEN2 was observed (Figure 8A).

Next, protein–protein interaction between *E. coli*–produced TON1b and *Arabidopsis* centrins was assayed in an in vitro pull-down assay. No association could be detected in the absence of calcium or with the glutathione *S*-transferase (GST) alone, while TON1b interacts directly with CEN1 and CEN2 when calcium is included in the reaction (Figure 8D).

To test whether TON1 and centrin are able to associate in vivo in the cellular context of plant cells, we performed bimolecular fluorescence complementation (BiFC) in *Nicotiana* leaf epidermal cells. In this assay, putative partners are fused to inactive N-terminal and C-terminal moieties of YFP (see Supplemental Figure 6 online). Bait and prey association brings YFP fragments together and drives reassembly of an active fluorescent protein, providing a direct readout of the interaction in vivo (Hu et al., 2002). As a control, GFP-TON1a, CEN1-GFP, and CEN2-GFP were expressed under the control of the 35S promoter. When transiently overexpressed, GFP-TON1a is present in the cytoplasm and does not label interphase MT arrays (Figure 8B). In these conditions, CEN1-GFP and CEN2-GFP also both accumulate in the cytoplasm and to a lesser extent in the nucleus (Figure 8B). Split-YFP fusions were constructed for TON1a, CEN1, and CEN2. For TON1a + CEN1, six out of eight combinations gave a positive signal (i.e., YFP fluorescence in the cytoplasm), with strong fluorescence in two cases (Figures 8B and 8C). For TON1a + CEN2, YFP complementation occurred with four combinations, but the signal was weaker than for TON1a–CEN1 interaction (Figures 8B and 8C). Therefore, TON1a is able to physically interact with both CEN1 and CEN2 in the cytoplasm of tobacco cells. Taken together, these results show that both CEN1 and CEN2 are able to physically interact with TON1a and b, both in vitro and in vivo.

To check whether these genes have overlapping expression patterns in *Arabidopsis*, we compared the transcription profiles of the TON1a and b and centrin genes with the Genevestigator tool (Zimmermann et al., 2004). TON1a, TON1b, CEN1, and FASS show similar expression patterns (see Supplemental Figure 3 online). They are transcribed in all organs and throughout

Figure 5. (continued).

(A) The N termini of several proteins belonging to various taxonomic groups were aligned. For clarity, only one representative sequence of each taxonomic group is shown here. Similarities are boxed, identities are in dark gray, and similarities are in light gray. Three highly conserved regions appear from the alignment: the TOF motif is located at the very beginning of all protein sequences. The second is a LisH dimerization motif (Emes and Ponting, 2001). A third region with a conserved PLL triad is presumably involved in LisH-mediated dimerization. Arrowheads indicate positions of deleterious mutations characterized in the human OFD1 gene (Romio et al., 2003).

(B) Phylogenetic tree of TON1 homologs. Multiple alignments of the ~180 N-terminal residues of each sequence were computed with Clustal, MAFFT, and Muscle algorithms (Thompson et al., 1994; Katoh et al., 2002; Edgar, 2004) and hand-curated to produce a consensus alignment. The alignment was used to produce an unrooted UPGMA tree. Bootstrap values are indicated on main branches (1000 repetitions). Four groups emerge from the N-terminal sequence alignment: land plant TON1, vertebrate FOP, vertebrate OFD, and a group of short (~175 residues) proteins related to FOP from various eukaryotes (FOP-like). The *Chlamydomonas* FOP is equally distant to TON1 and FOP. At, *Arabidopsis thaliana*; Os, *Oryza sativa*; Pi, *Pinus tadea*; Cy, *Cycas rumphii*; Pp, *Physcomitrella patens*; Hs, *Homo sapiens*; Gg, *Gallus gallus*; Xl, *Xenopus laevis*; Dr, *Danio rerio*; Ci, *Ciona Intestinalis*; Cr, *Chlamydomonas reinhardtii*; Tn, *Tetraodon nigroviridis*; Nv, *Nematostella vectensis*; Pt, *Paramecium tetraurelia*; Lm, *Leishmania majo*; Tb, *Trypanosoma brucei*; Am, *Apis mellifera*; Tv, *Trichomonas vaginalis*; Gl, *Giardia lamblia*. Accession numbers are listed in Supplemental Figure 4 online.

(C) Comparison of TON1 and FOP reveals a similar organization at their N terminus, with conserved motifs described above, a short Ser-rich region (S), and Ser phosphorylation sites (Benschop et al., 2007) around positions 150 to 160. FOP also has a Tyr phosphorylation site at position 337 (http://www.phosphosite.org/).

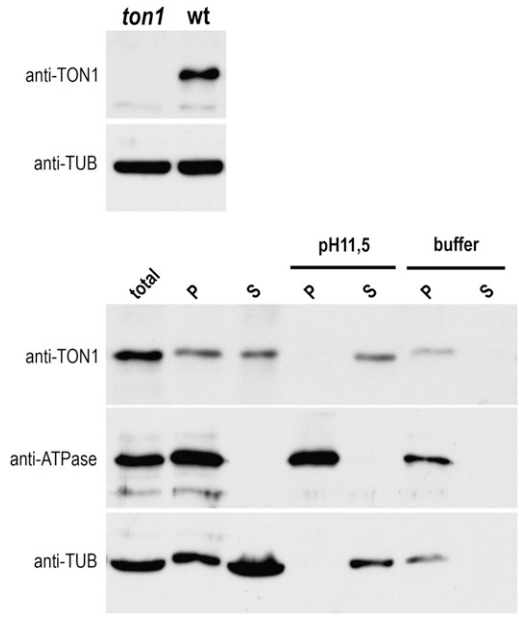

Figure 6. Subcellular Localization of the TON1 Proteins.

Top panel: Protein gel blot analysis of total proteins of *ton1* and wild-type 10-d-old in vitro–grown seedlings probed against the anti-TON1 polyclonal serum and an anti-α-tubulin antibody. TON1 proteins are undetectable in the *ton1* mutant extract. Bottom panel: Total proteins and proteins from soluble (S) and pellet (P) fractions obtained from adult rosette leaves were separated by electrophoresis, transferred to membrane, and probed with anti-TON1 serum, anti-α-tubulin antibody, and anti-H^+-ATPase serum. Upon exposure to high pH (pH 11.5), TON1 proteins were released from the pellet fraction and solubilized, whereas resuspension of the pellet in the homogenization buffer used to make the original protein extract did not. As a control, the intrinsic membrane protein H^+-ATPase is not released from membranes after exposure to high pH. Size of the proteins is as follows: TON1, 30 kD; tubulin, 50 kD; H^+-ATPase, 100 kD.

development. They are all highly expressed in actively dividing cells, such as cell culture and callus, and display no periodicity during the cell cycle in synchronized cells. Moreover, these genes are essentially not responsive to most biotic and abiotic stimuli. We conclude that these genes are constitutively expressed, consistent with a housekeeping role. CEN2 expression is different: it is exclusively expressed in roots and senescent leaves, not expressed in cell culture, and its expression is highly responsive to a series of biotic and abiotic treatments. Added to the documented role of CEN2 in genotoxic stress response (Molinier et al., 2004) and absence of interaction of CEN2 with TON1b in yeast, expression data suggest that CEN1 is the bona fide partner of TON1 in vivo.

DISCUSSION

The *ton1* and *fass*/*ton2* are the only viable mutations known to totally suppress formation of the PPB in plant cells. Very few other mutations, such as maize *tangled* (Cleary and Smith, 1998) or *Arabidopsis mor1* (Kawamura et al., 2006), are known to specifically affect this structure. Even though most cellular and developmental defects in *ton1* mutants may be interpreted as more or less direct consequences of this absence of PPB and subsequent mispositioning of division planes, several lines of evidence point to an involvement of TON1a and b in all cortical arrays, not only during G2/M transition and PPB formation, but also during interphase and cell elongation: (1) the interphase MT arrays and anisotropic growth are strongly disturbed in the mutant; (2) a GFP-TON1a fusion labels the interphase array; (3) consistent with a role at the cell cortex during interphase, we detected TON1 in a membrane-associated pool in extracts from whole plants, and both TON1a and b were present in cortical extracts from cultured cells (Benschop et al., 2007); (4) the transcription pattern of both TON1a and b suggests a housekeeping activity, and the absence of significant cyclic transcript variation during the cell cycle does not favor a purely mitotic role. Taken together, these results point to a general role of TON1 in formation and/or maintenance of all cortical arrays of MTs. Given its biochemical features and the labeling pattern we observe, it seems unlikely that TON1 is capable of direct interaction with MTs. This targeting could be brought about by other TON1 potential interactors recovered from our two-hybrid screen, which possess large basic domains, a common feature of microtubule-associated proteins (S. Drevensek, unpublished results).

The similarity of *ton1* and *fass*/*ton2* morphological, cellular, and cytoskeletal defects strongly suggest that they are part of a same pathway. FASS encodes a PP2A regulatory subunit (Camilleri et al., 2002) and as such is expected to be responsible for the subcellular targeting and substrate specificity of a PP2A phosphatase activity. In *Caenorhabditis elegans*, the FASS homolog has been recently shown to target a PP2A complex to the centrosome for mitotic spindle assembly (Schlaitz et al., 2007). In a recent study, TON1a was shown to associate in vivo with *Arabidopsis* CDKA;1 (Van Leene et al., 2007), providing an interesting link between TON1's function and the cell cycle machinery. CDK is indeed known from several studies to transiently associate with the PPB in plant cells (Weingartner et al., 2001). In animal cells, the initial activation of cyclin B1-Cdk1 in early prophase takes place at the centrosome, before spreading into the cell for entry into mitosis (Jackman et al., 2003).

A possible role for TON1 could be to recruit these kinase and phosphatase activities at the cortical cytoskeleton to regulate assembly/disassembly of the cortical arrays of MTs. As TON1a and TON1b are phosphorylated in *Arabidopsis* (Benschop et al., 2007; Sugiyama et al., 2008), TON1 could alternatively/additionally be a target for FASS-dependent dephosphorylation. In plants, several lines of evidence implicate reversible protein phosphorylation in the regulation of the plant MT cytoskeleton, including PPB formation (Baskin et al., 1999; Ayaydin et al., 2000).

A proteomics survey of the human interphase centrosome identified a total of 83 centrosomal proteins as well as 41 likely candidates (Andersen et al., 2003). Apart from γ-TuRC components (Pastuglia and Bouchez, 2007) and tubulins, few of these >120 proteins have clear homologs in *Arabidopsis*, including

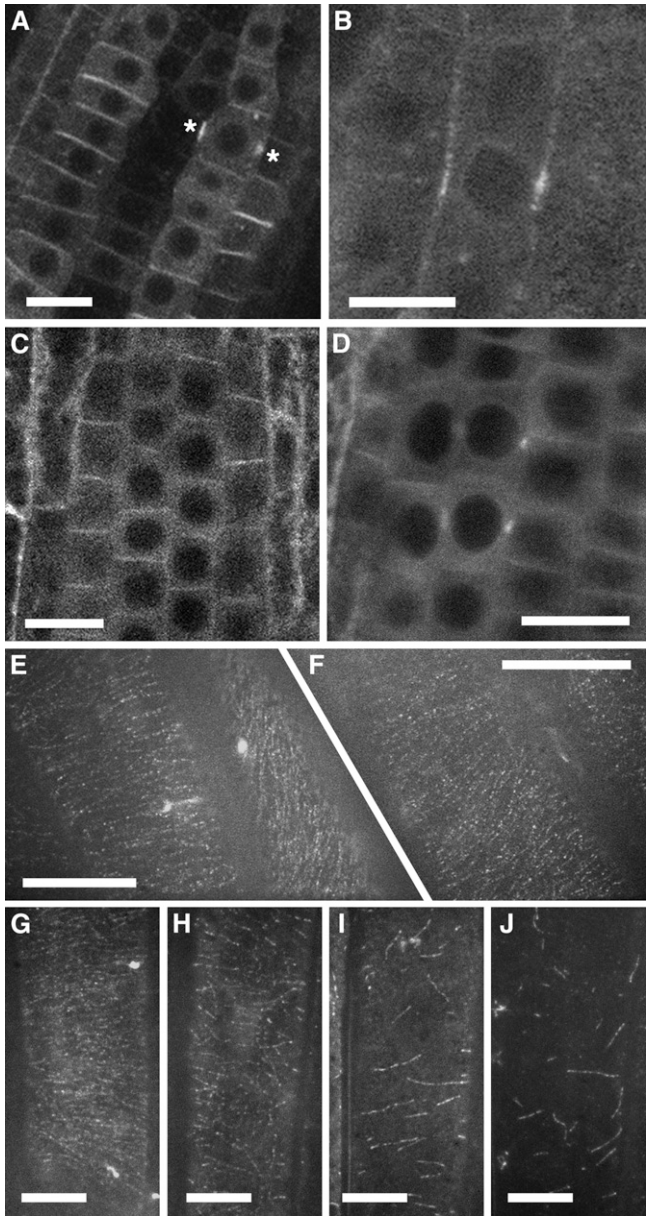

Figure 7. Localization of a GFP-TON1 Fusion in *Arabidopsis* and Tobacco Cells.

(A) and **(B)** In the *Arabidopsis* root tip of 5-d-old seedlings, in addition to a cytoplasmic staining, the GFP-TON1a fusion faintly but consistently labels the PPB (asterisk in **[A]** and cell in **[B]**). In actively dividing cell files, GFP-TON1a also accumulates on the transverse sides of cells **(A)**.

(C) and **(D)** The same pattern is observed in transformed tobacco roots expressing GFP-TON1a; see labeled cross-wall in **(C)** and two cells displaying PPB in **(D)**.

(E) and **(F)** In *Arabidopsis* expanding hypocotyl cells of 3-d-old etiolated seedlings, GFP-TON1a accumulates as discrete punctate staining organized into dense linear arrays, reminiscent of MT organization in expanding cells. Usually, most of expanding hypocotyls cells display MT arrays roughly transverse to the cell axis similar to the GFP-TON1a staining seen in the left cell in **(E)** and in **(F)**, although some cells can have more longitudinal arrays as the right cell in **(E)** (similar patterns are described in Paredez et al., 2006; Chan et al., 2007).

CDK and centrin. Therefore, the sequence similarity between plant TON1a and b proteins and two human centrosomal proteins is noteworthy. Both FOP and OFD1 are highly conserved in the vertebrate lineage. FOP was originally identified from a human stem cell myeloproliferative syndrome (Popovici et al., 1999) and localizes to the human centrosome (Andersen et al., 2003; Yan et al., 2006). FOP is phosphorylated in a cell cycle–dependent manner in human cells and retains its centrosome localization during cell division in U2OS cells (Yan et al., 2006), as opposed to TON1, which seems not associated with mitotic structures. Interestingly, the positions of FOP and TON1 phosphorylation sites are similar, next to the LisH/PLL dimerization region (Figure 5). As for OFD1, mutations in this protein cause polycystic kidney disease and malformations of the mouth, face, and digits. This protein, rich in coiled-coil segments, is expressed in several cell types and lineages during development and also localizes to the centrosome (Andersen et al., 2003; Romio et al., 2003). Genetic studies of human patients reveal that several deleterious mutations map to the N terminus, including mutations in the LisH motif (Figure 5).

A further element connecting TON1a and b to centrosomes is its interaction with centrin. Numerous studies in lower and higher eukaryotes have established a key role for centrin in the dynamic behavior of centrosomes, through control of the cohesion of centrosomal structures and duplication of the centriole/basal body (Salisbury et al., 2002). Centrin is present in the whole green lineage from algae to angiosperms. Both the expression profile and the subcellular localization of CEN1 are overlapping with those of TON1a and b: in plant cells, fractionation and localization studies consistently identified a membrane-associated centrin pool (DelVecchio et al., 1997; Blackman et al., 1999; Stoppin-Mellet et al., 1999; Harper et al., 2000). Moreover, in recent proteomic studies, CEN1 and TON1a and b were all found associated with the cortex (Benschop et al., 2007). By contrast, CEN2 was not detected in this study, and its transcription profile is not in favor of an interaction with TON1a or b in vivo. CEN2 has been shown to modulate homologous recombination and nucleotide excision repair in *Arabidopsis* (Molinier et al., 2004) and to localize to the nucleus upon UV-C treatment (Liang et al., 2006). Therefore, on the basis of its expression and localization, CEN1 is a better candidate for interaction with TON1. TON1a and b interact with both CEN1 and CEN2 in BiFC and in vitro, but contrary to CEN1, CEN2 does not bind TON1b in yeast two-hybrid experiments. This difference in yeast may reflect divergence of *Arabidopsis* centrins at a PKA phosphorylation site present in CEN2 but not in CEN1 (Figure 8E), a site known in *Chlamydomonas* to modulate the structure and biochemical activities of centrin (Meyn et al., 2006). In human HeLa cells,

(G) to **(J)** *Arabidopsis* hypocotyl cells expressing GFP-TON1a before **(G)** and after incubation in 10 μM oryzalin for 5 min **(H)**, 15 min **(I)**, and 70 min **(J)**. Micrographs in **(A)** to **(D)** are confocal laser scanning microscope images, and images in **(E)** to **(J)** were obtained using a spinning disk confocal microscope. All plantlets express the GFP-TON1a fusion under the control of the 35S promoter. Bars = 20 μm in **(A)**, **(C)**, and **(D)** to **(F)** and 10 μm in **(B)** and **(G)** to **(J)**.

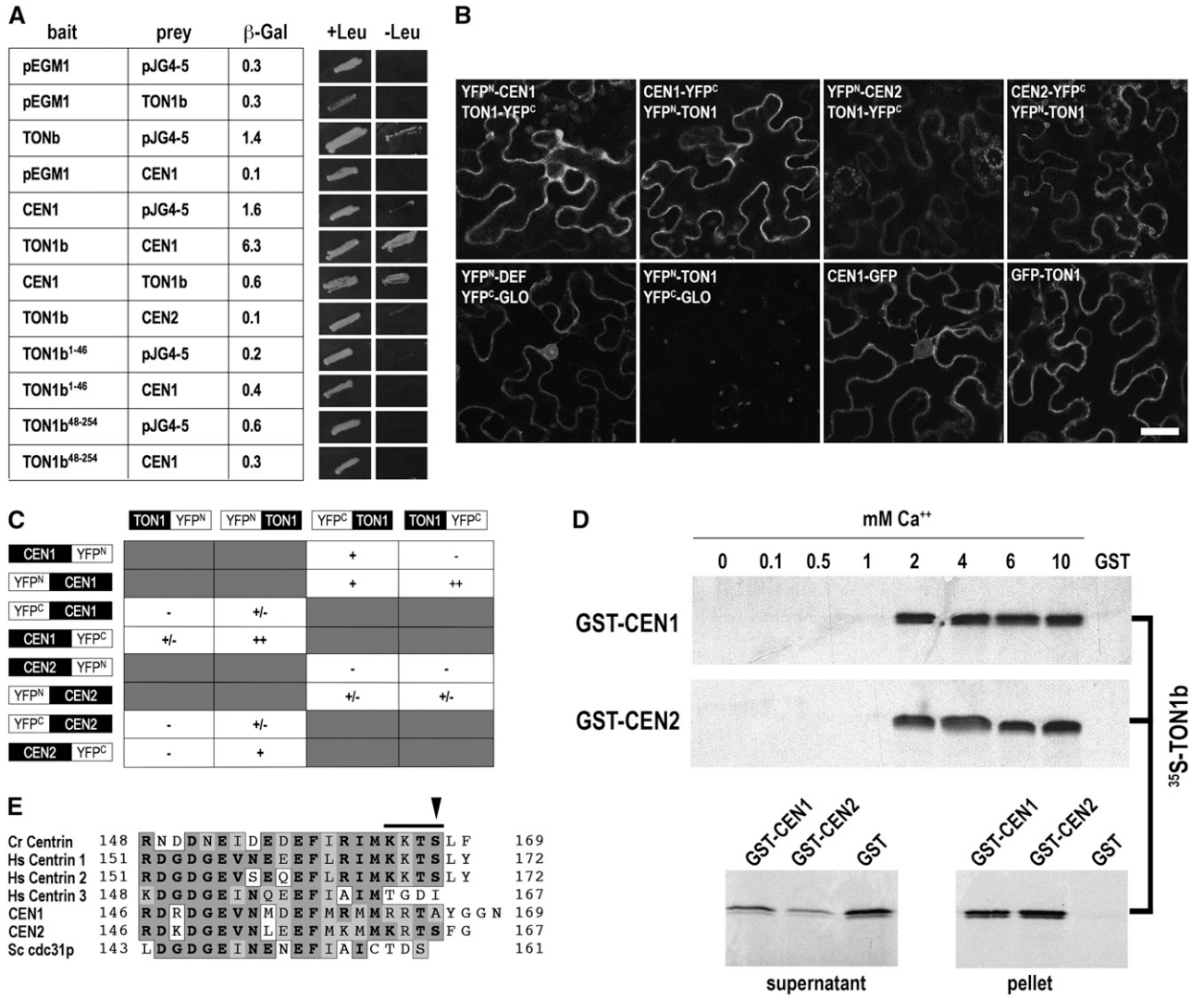

Figure 8. Interaction of TON1 with *Arabidopsis* Centrins.

(A) Yeast two-hybrid experiments. Bait TON1b fragments and CEN1 were cloned as LexA fusions; pEGM1 and pJG4-5 are empty vector controls. Full-length TON1b, CEN1, and CEN2 prey fragments were cloned in pJG4-5. β-Gal activity is expressed in arbitrary units. Left panels: Growth of yeast cells on nonselective medium with Leu (+Leu). Right panels: Growth of yeast clones on selective medium without Leu (−Leu). The LEU2 reporter in EGY48 is known to be more sensitive than the β-Gal reporter for some baits (Ausubel et al., 1998), which may explain the low level of β-Gal for CEN1-TON1b compared with its growth on −Leu medium.

(B) BiFC visualization of TON1a interaction with *Arabidopsis* centrins. Shown are confocal images of tobacco epidermal cells coinfiltrated with *Agrobacterium* cultures harboring expression vectors. In the typical jigsaw puzzle cells, the cytoplasm and nucleus are restricted to the cell's periphery by the large central vacuole. When transiently overexpressed under the control of the 35S promoter, CEN1-GFP localizes to the cytoplasm and the nucleus (bottom panel, middle right), and GFP-TON1 localizes to the cytoplasm (bottom panel, right). Positive control for the BiFC experiment corresponds to coexpression of YFP^N-DEF and YFP^C-GLO (bottom panel, left), the documented heterodimeric complex formation between *Anthirrinum majus* MADS box transcription factors DEFICIENS and GLOBOSA (Schwarz-Sommer et al., 1992). Negative controls correspond to expression of the protein of interest (TON1 or CEN1 or 2) fused to YFP moiety alone or to coexpression of these protein fusions with unrelated proteins (i.e., DEFICIENS and GLOBOSA). Here, coexpression of YFP^N-TON1 and YFP^C-GLO is shown (bottom panel, middle left). Top panels correspond to examples of YFP complementation obtained after coexpression of the indicated fusion proteins. As expected in these conditions of strong overexpression, the location of TON1-centrin complexes formation is cytoplasmic. Bar = 25 μm.

(C) Summary of interactions between TON1a and *Arabidopsis* centrins, CEN1 and CEN2, assayed by BiFC in epidermal cells of *N. benthamiana*. ++, strong fluorescent signal; +, significant fluorescent ± weak signal above background; −, no significant signal.

(D) In vitro pull-down assays. CEN1 and CEN2 were produced in *E. coli* as fusions with the GST glutathione binding domain. ^{35}S-TON1b was produced in vitro in a coupled transcription/translation system. Top panels: The GST fusions were bound on gluthathione-agarose, washed and incubated with ^{35}S-TON1b in the presence of increasing concentrations of Ca^{2+} (from 0 to 10 mM), before elution and analysis by SDS-PAGE and autoradiography. GST, negative control (GST alone, 10 mM Ca^{2+}). Bottom panels: Experiment showing the supernatant (left) and pellet (right) of a ^{35}S-TON1b pull-down assay with GST-CEN1, GST-CEN2, and GST alone under 10 mM Ca^{2+}.

(E) Amino acid alignment of the C-terminal part of *Chlamydomonas reinhardtii* centrin, human centrins 1, 2, and 3, *Arabidopsis* CEN1 and CEN2, and yeast cdc31p, showing differences at a C-terminal phosphorylation site for cAMP-dependent protein kinase ([R/K]-[R/K]-x-[S/T]; bar) and presence of a phosphorylatable Ser (arrowhead). Similarities are boxed, and identities are in bold.

centrin phosphorylation occurs at the G2/M transition (Lutz et al., 2001), a stage that overlaps with PPB occurrence in plant cells.

Centrin is an EF-hand calcium binding protein closely related to the ubiquitous calcium sensor calmodulin. Although the functional significance of TON1–centrin interaction needs to be further clarified, the calcium-dependent binding of this protein to TON1 could modulate its localization, activity, or affinity for other partners.

Vertebrate centrosomes are involved in a range of cellular events in addition to their MT organizing center activity for the formation of interphase cytoplasmic MT arrays, mitotic spindles, or cilia (Rieder et al., 2001). They are notably involved in cell cycle transitions, cellular responses to stress, and organization of signal transduction pathways (Doxsey et al., 2005). The similarity of the N-terminal parts of TON1a and b and two human centrosomal proteins, precisely in a region shown to be important for their targeting and function at the centrosome, as well as the interaction of TON1a and b with *Arabidopsis* centrin, raise the interesting possibility that, in addition to γ-tubulin–dependent MT nucleation, other functions and molecular networks involved in the organization of MT arrays by the centrosome were conserved across the evolutionary divergence between plants and animals. The location of such centrosomal players at the cortex of plant cells is consistent with the view of the cell cortex as the flexible centrosome of plant cells (Mazia, 1984), involved in nucleation, release, and attachment of MTs at the membrane's periphery (Ehrhardt and Shaw, 2006). TON1a and b could participate in such centrosome-like functions at the cortex of plant cells, for example, by recruiting regulatory complexes involved in the regulation of cytoskeleton arrays in connection with the cell cycle.

METHODS

Plant Material and Growth Conditions

A single mutant allele was isolated for the *ton1* locus (Traas et al., 1995), segregating in line ACL4, originally obtained from large-scale T-DNA insertional mutagenesis in ecotype Ws (Bechtold et al., 1993). For the synonymous *fass* (Mayer et al., 1991) and *ton2* (Traas et al., 1995; Camilleri et al., 2002) locus, the consensual name is now *fass* (synonym: *ton2*). *Arabidopsis thaliana* plants were grown in vitro or in the greenhouse as described previously (Nacry et al., 1998). The GFP-MBD marker in *Arabidopsis* (Camilleri et al., 2002) was introduced in the *ton1* mutant background by crossing.

Clones and Primers

A full-length TON1b clone was isolated from an *Arabidopsis* cDNA library (L*er* ecotype) and fully sequenced. A full-length cDNA clone for TON1a (AV539220) was obtained from the Kazusa DNA Research Institute (Japan). A rice (*Oryza sativa*) cDNA clone (D39592) highly related to TON1 was obtained from the Rice Genome Research Program (Japan) and fully sequenced. Oligonucleotides used in this study are as follows: TON1a and TON1b gene-specific primers Spec1aF (5′-TAGTTCAAGGAGAGATTCAGAAACA-3′), Spec1aR (5′-CAATTCAAGGCTCAGAAGGATAGT-3′), Spec1bF (5′-ATATTTGGACTGGGCGCAATTA-3′), Spec1bR (5′-CAGAAGAAGCGGTCTAC-3′); APT1 primers APT-RT1 (5′-TCCCAGAATCGCTAAGATTGCC-3′) and APT-RT2 (5′-CCTTTCCCTTAAGCTCTG-3′).

Molecular Cloning Techniques

Cloning and sequencing procedures were performed essentially as described by Nacry et al. (1998). RT-PCR analyses were performed as described by Camilleri et al. (2002) using the following primers: Spec1aF and Spec1aR for *TON*1a cDNA and Spec1bF and Spec1bR for *TON*1b cDNA. APT1 cDNA was used as an internal control (Moffatt et al., 1994) and was amplified using primers APT-RT1 and APT-RT2.

Two-Hybrid Experiments

A LexA-TON1b fusion protein was used as a bait to screen a cDNA library from *Arabidopsis* young siliques as described (Grebe et al., 2000). Materials and experimental procedures for screening, quantitative β-Gal assays, and plasmid isolation were essentially as described (Ausubel et al., 1998). More than 3.10^6 independent transformants were obtained, and 20.10^6 cells from this pool were replated on Leu- selection medium. Yeast colonies growing on selection plates were screened for β-Gal activity. A total of 250 Leu+ clones that showed β-Gal activity were selected for further analysis. Prey plasmids were isolated from positive clones and reintroduced into yeast strain EGY48, either alone or with the bait plasmid, and reassayed for growth on selective medium and quantitation of β-Gal activity.

GFP and BiFC Constructs

All *Arabidopsis* open reading frames flanked by AttB1 and AttB2 sites were amplified from *Arabidopsis* cDNA clones (Columbia ecotype), cloned into Gateway vector pDONR207 using BP recombination (Invitrogen), and sequenced. To obtain the plasmid carrying a GFP-TON1a fusion under the control of the 35S promoter, pDONR207:TON1a was used in a LR reaction with destination vector pGWB6 (kind gift of T. Nakagawa, Shimane University, Japan). PTON1a-GFP-TON1a comprises 1.1 kb of TON1a promoter driving a GFP-TON1a fusion protein. Globosa and Deficiens entry clones were provided by B. Davies (University of Leeds, UK). An LR reaction between the entry vector and the complete set of four pBiFP vectors (see Supplemental Figure 6 online) produced the final expression vectors, where coding sequences are cloned in fusion with the N- and C-terminal parts of YFP, either as N-terminal or C-terminal fusions, under the control of the cauliflower mosaic virus 35S promoter. For fluorescence complementation tests, all eight compatible combinations between protein pairs (i.e., providing both parts of the YFP) were assayed in transient expression.

Transient Assay in *Nicotiana benthamiana* Leaves

Each expression vector was introduced in *Agrobacterium tumefaciens* strain C58C1(pMP90) by electroporation. *Agrobacterium* bacterial cultures were incubated overnight at 28°C with agitation. Each culture was pelleted, washed, and resuspended in infiltration buffer (13 g/L bouturage N°2 medium [Duchefa Biochemie] and 40 g/L sucrose, pH 5.7) to an OD_{600} of 0.5. The inoculum was delivered to the lamina tissue of *N. benthamiana* leaves by gentle pressure infiltration through the lower epidermis. To enhance transient expression of GFP and BiFC fusion proteins, the P19 viral suppressor of gene silencing was coexpressed (Voinnet et al., 2003). For coexpression experiments, equal volumes of each bacterial culture (OD_{600} of 0.5) were mixed before infiltration. YFP or GFP fluorescence was detected 2 to 3 d after infiltration.

Plant Transformation

Arabidopsis plants were transformed using the vacuum infiltration protocol (Bechtold et al., 1993). Transformed tobacco roots were obtained by coinoculation of *Nicotiana tabacum* (Xanthi XHFD8) leaf disks with

Agrobacterium rhizogenes A4 and *A. tumefaciens* C58C1(pMP90) harboring the expression vector. After coculture on Murashige and Skoog (MS) medium (3 d, 24°C, dark), leaf disks were transferred on solid MS medium containing kanamycin (50 mg/L) and cefotaxim (500 mg/L) and grown in the dark at 24°C with 50% humidity. After 4 weeks, hairy-root clones were individually transferred to fresh medium and cultured for 4 weeks. They were transferred to liquid MS medium with no antibiotic for 1 week before analysis by confocal microscopy.

Immunofluorescence and Microscopy

Tubulin immunostaining of wild-type and *ton1* seedlings was performed as described previously (Pastuglia et al., 2006). Except for GFP-TON1a localization in hypocotyls cells, all images (immunolocalization studies and GFP and BiFC experiments) were obtained using a Leica SP2 AOBS confocal laser scanning microscope. Optical sections were collected with a Leica HCX PL APO ×63/1.20 NA water objective upon illumination of the sample with a 488-nm argon laser line. GFP-TON1a localization in expanding hypocotyls cells was performed using a spinning disk confocal Revolution XD from Andor Technology mounted on an inverted Axiovert 200M microscope from Carl Zeiss. The system employs a Yokogawa CSU22 confocal spinning disk unit, a solid-state laser line (488 nm) controlled by acousto-optic tuneable filter (AOTF), and a EM-CCD camera DV885 from Andor Technology using a ×100 Apochromat NA1.4 oil immersion objective (Carl Zeiss). Images were processed using ImageJ software (NIH).

Expression of Recombinant TON1b and Immunological Techniques

A His tagged-TON1b fusion protein was cloned in pET14 and expressed in *Escherichia coli* cells. Inclusion bodies, containing the recombinant protein, were solubilized in lysis buffer (8 M urea, 10 mM Tris, pH 8, 100 mM NaCl, and 50 mM Na_2HPO_4, pH8) and affinity-purified using TALON metal affinity resin as indicated by the supplier (Clontech). Lysis buffer was exchanged for 3 M urea, 0.2% Triton X-100 in dilution buffer (50 mM Tris, pH 8, 0.5 mM EDTA, 50 mM NaCl, and 5% glycerol), and purified recombinant protein was refolded by serial dilutions in dilution buffer supplemented with 0.2% Triton X-100. Refolded recombinant protein was concentrated using a Centriprep 10 concentrator (Amicon) and used to produce a rabbit antiserum following the standard immunization protocols of Biogenes.

Immunoblots were performed on Hybond C membranes (Amersham) with a 1:1000 dilution of the anti-TON1b rabbit antibody, a 1:5000 dilution of a rabbit polyclonal serum raised against *Nicotiana plumbaginifolia* H^+-ATPase (Morsomme et al., 1998), or a 1:5000 dilution of a monoclonal anti-α-tubulin antibody (clone B5-1-2; Sigma-Aldrich). Secondary antibodies were anti-rabbit or anti-mouse IgG linked to horseradish peroxydase (Sigma-Aldrich). Signals were revealed using the Amersham ECL system.

Cell Fractionation and Preparation of *Arabidopsis* Protein Extracts

For preparation of total plant extracts, seedlings were frozen in liquid nitrogen and ground; the powder was resuspended in SDS-PAGE Laemmli buffer. The samples were centrifuged at 10,000*g* to remove any remaining tissue, and the supernatant was retained for electrophoresis.

Membrane and soluble protein fractions were obtained essentially as described by Santoni (2007). Leaves of 4-week-old plants were disrupted at 4°C in a Waring blender in homogenization buffer (500 mM sucrose, 50 mM Tris-HCl, 20 mM EDTA, 20 mM EGTA, 10% glycerol, 10 mM ascorbic acid, 0.5% polyvinylpyrrolidone, 5 mM DTT, 1 mM Na_3VO_4, 1 mM Na_2MoO_4, 50 mM $Na_4P_2O_7$, 1 mM AEBSF, 1 μg/mL leupeptine, and 1 μg/mL pepstatine A, pH adjusted to 8 with MES) for 10 s at low speed and four times for 10 s at high speed. The homogenization buffer-to-tissue ratio was 2 mL buffer/g fresh weight. An aliquot of the homogenate was resuspended in SDS-PAGE sample for electrophoresis of total protein extracts. The remaining homogenate was filtrated through two layers of Miracloth (Calbiochem) and then centrifuged at 26,000*g* max for 25 min. The supernatant was then centrifuged at 84,000*g* max for 25 min to recover the microsomal fraction, and the supernatant was retained for the soluble protein fraction. For electrophoresis, the proteins (microsomal and soluble fractions) were resuspended in SDS-PAGE sample buffer. For stripping of membrane-associated proteins, the microsomal fraction was resuspended at 4°C for 1 h either in 100 mM Na_2CO_3, pH 11.5, or in homogenization buffer alone or supplemented with 1% Triton X-100 or 0.5% CHAPS. After centrifugation at 84,000*g* max for 25 min, the pellets and supernatants were solubilized in SDS-PAGE sample buffer.

Accession Numbers

Sequence data from this article can be found in the Arabidopsis Genome Initiative under the following accession numbers: TON1a, At3g55000; TON1b, At3g55005; CEN1, At3g50360; CEN2, At4g37010; CDKA;1, At3g48750; and APT1, At1g27450. Sequences obtained in this work can be found in the GenBank/EMBL databases under the following accession numbers: TON1 locus, AF280058; TON1b cDNA, AF280059; and rice TON1 cDNA, AF280060.

Supplemental Data

The following materials are available in the online version of this article.

Supplemental Figure 1. Complex Chromosomal Rearrangement in the ACL4 Line.

Supplemental Figure 2. Both TON1a and TON1b Genes Complement the *ton1* Mutation, and Overexpression of Either TON1a or TON1b Does Not Induce a Morphological Phenotype in a Wild-Type Background.

Supplemental Figure 3. Affymetrix Transcriptome Data for TON1a, TON1b, CEN1, CEN2, and FASS.

Supplemental Figure 4. Intron Position Is Conserved in TOF-Containing Proteins.

Supplemental Figure 5. The GFP-TON1 Fusion Displays the Typical Organization of a PPB.

Supplemental Figure 6. BiFC Vectors.

Supplemental Data Set 1. Alignment from Figure 5 in FASTA Format.

ACKNOWLEDGMENTS

We thank V. Santoni, G. Ephritikine, R. Cyr, and B. Davies for providing materials used in this work. We thank B. Courtial and O. Grandjean for their help and G. Jürgens for the gift of the two-hybrid library. Spinning-disk confocal imaging was performed at Plate-Forme d'Imagerie Dynamique (Institut Pasteur) with the help of C. Machu. J.A., P.N., and S.D. were recipients of fellowships from the French Ministry for Research, and A.C. was a recipient of an E.U. Marie Curie Fellowship. This work was supported by grants from the French Ministry for Research.

Received November 27, 2007; revised July 29, 2008; accepted July 31, 2008; published August 29, 2008.

REFERENCES

Andersen, J.S., Wilkinson, C.J., Mayor, T., Mortensen, P., Nigg, E.A., and Mann, M. (2003). Proteomic characterization of the human centrosome by protein correlation profiling. Nature **426:** 570–574.

Ausubel, F.M., Brent, R., Kingston, R.E., Moore, D.D., Seidman, J.G., Smith, J.A., and Struhl, K. (1998). Current Protocols in Molecular Biology. (New York: John Wiley & Sons).

Ayaydin, F., Vissi, E., Meszaros, T., Miskolczi, P., Kovacs, I., Feher, A., Dombradi, V., Erdodi, F., Gergely, P., and Dudits, D. (2000). Inhibition of serine/threonine-specific protein phosphatases causes premature activation of cdc2MsF kinase at G2/M transition and early mitotic microtubule organisation in alfalfa. Plant J. **23:** 85–96.

Baskin, T.I., Meekes, H.T.H.M., Liang, B.M., and Sharp, R.E. (1999). Regulation of growth anisotropy in well-watered and water-stressed maize roots. II. Role of cortical microtubules and cellulose microfibrils. Plant Physiol. **119:** 681–692.

Bechtold, N., Ellis, J., and Pelletier, G. (1993). In planta Agrobacterium mediated gene transfer by infiltration of adult *Arabidopsis thaliana* plants. C. R. Acad. Sci. III **316:** 1194–1199.

Benschop, J.J., Mohammed, S., O'Flaherty, M., Heck, A.J., Slijper, M., and Menke, F.L. (2007). Quantitative phosphoproteomics of early elicitor signaling in Arabidopsis. Mol. Cell. Proteomics **6:** 1198–1214.

Blackman, L.M., Harper, J.D., and Overall, R.L. (1999). Localization of a centrin-like protein to higher plant plasmodesmata. Eur. J. Cell Biol. **78:** 297–304.

Buschmann, H., Chan, J., Sanchez-Pulido, L., Andrade-Navarro, M. A., Doonan, J.H., and Lloyd, C.W. (2006). Microtubule-associated AIR9 recognizes the cortical division site at preprophase and cell-plate insertion. Curr. Biol. **16:** 1938–1943.

Camilleri, C., Azimzadeh, J., Pastuglia, M., Bellini, C., Grandjean, O., and Bouchez, D. (2002). The Arabidopsis TONNEAU2 gene encodes a putative novel PP2A regulatory subunit essential for the control of cortical cytoskeleton. Plant Cell **14:** 833–845.

Chan, J., Calder, G., Fox, S., and Lloyd, C. (2007). Cortical microtubule arrays undergo rotary movements in Arabidopsis hypocotyl epidermal cells. Nat. Cell Biol. **9:** 171–175.

Cleary, A.L., and Smith, L.G. (1998). The Tangled1 gene is required for spatial control of cytoskeletal arrays associated with cell division during maize leaf development. Plant Cell **10:** 1875–1888.

Dammermann, A., Desai, A., and Oegema, K. (2003). The minus end in sight. Curr. Biol. **13:** R614–R624.

DelVecchio, A.J., Harper, J.D.I., Vaughn, K.C., Baron, A.T., Salisbury, J.L., and Overall, R.L. (1997). Centrin homologues in higher plants are prominently associated with the developing cell plate. Protoplasma **196:** 224–234.

Dixit, R., and Cyr, R. (2004). The cortical microtubule array: From dynamics to organization. Plant Cell **16:** 2546–2552.

Doxsey, S., McCollum, D., and Theurkauf, W. (2005). Centrosomes in cellular regulation. Annu. Rev. Cell Dev. Biol. **21:** 411–434.

Edgar, R.C. (2004). MUSCLE: Multiple sequence alignment with high accuracy and high throughput. Nucleic Acids Res. **32:** 1792–1797.

Ehrhardt, D.W., and Shaw, S.L. (2006). Microtubule dynamics and organization in the plant cortical array. Annu. Rev. Plant Biol. **57:** 859–875.

Emes, R.D., and Ponting, C.P. (2001). A new sequence motif linking lissencephaly, Treacher Collins and oral-facial-digital type 1 syndromes, microtubule dynamics and cell migration. Hum. Mol. Genet. **10:** 2813–2820.

Ferrante, M.I., et al. (2001). Identification of the gene for oral-facial-digital type I syndrome. Am. J. Hum. Genet. **68:** 569–576.

Graham, L. (1996). Green algae to land plants: an evolutionary transition. J. Plant Res. **109:** 241–251.

Grebe, M., Gadea, J., Steinmann, T., Kientz, M., Rahfeld, J.U., Salchert, K., Koncz, C., and Jurgens, G. (2000). A conserved domain of the arabidopsis GNOM protein mediates subunit interaction and cyclophilin 5 binding. Plant Cell **12:** 343–356.

Harper, J.D.I., Fowke, L.C., Gilmer, S., Overall, R.L., and Marc, J. (2000). A centrin homologue is localised across the developing cell plate in gymnosperms and angiosperms. Protoplasma **211:** 207–216.

Hu, C.D., Chinenov, Y., and Kerppola, T.K. (2002). Visualization of interactions among bZIP and Rel family proteins in living cells using bimolecular fluorescence complementation. Mol. Cell **9:** 789–798.

Jackman, M., Lindon, C., Nigg, E.A., and Pines, J. (2003). Active cyclin B1-Cdk1 first appears on centrosomes in prophase. Nat. Cell Biol. **5:** 143–148.

Katoh, K., Misawa, K., Kuma, K., and Miyata, T. (2002). MAFFT: A novel method for rapid multiple sequence alignment based on fast Fourier transform. Nucleic Acids Res. **30:** 3059–3066.

Kawamura, E., Himmelspach, R., Rashbrooke, M.C., Whittington, A. T., Gale, K.R., Collings, D.A., and Wasteneys, G.O. (2006). MICROTUBULE ORGANIZATION 1 regulates structure and function of microtubule arrays during mitosis and cytokinesis in the Arabidopsis root. Plant Physiol. **140:** 102–114.

Liang, L., Flury, S., Kalck, V., Hohn, B., and Molinier, J. (2006). CENTRIN2 interacts with the Arabidopsis homolog of the human XPC protein (AtRAD4) and contributes to efficient synthesis-dependent repair of bulky DNA lesions. Plant Mol. Biol. **61:** 345–356.

Lloyd, C., and Chan, J. (2004). Microtubules and the shape of plants to come. Nat. Rev. Mol. Cell Biol. **5:** 13–22.

Lutz, W., Lingle, W.L., McCormick, D., Greenwood, T.M., and Salisbury, J.L. (2001). Phosphorylation of centrin during the cell cycle and its role in centriole separation preceding centrosome duplication. J. Biol. Chem. **276:** 20774–20780.

Mayer, Y., Torres Ruiz, R.A., Berleth, T., Misera, S., and Jurgens, G. (1991). Mutations affecting body organization in the Arabidopsis embryo. Nature **353:** 402–407.

Mazia, D. (1984). Centrosomes and mitotic poles. Exp. Cell Res. **153:** 1–15.

McClinton, R.S., and Sung, Z.R. (1997). Organization of cortical microtubules at the plasma membrane in Arabidopsis. Planta **201:** 252–260.

Menges, M., Hennig, L., Gruissem, W., and Murray, J.A. (2003). Genome-wide gene expression in an Arabidopsis cell suspension. Plant Mol. Biol. **53:** 423–442.

Meyn, S.M., Seda, C., Campbell, M., Weiss, K.L., Hu, H., Pastrana-Rios, B., and Chazin, W.J. (2006). The biochemical effect of Ser167 phosphorylation on *Chlamydomonas reinhardtii* centrin. Biochem. Biophys. Res. Commun. **342:** 342–348.

Mikolajka, A., Yan, X., Popowicz, G.M., Smialowski, P., Nigg, E.A., and Holak, T.A. (2006). Structure of the N-terminal domain of the FOP (FGFR1OP) protein and implications for its dimerization and centrosomal localization. J. Mol. Biol. **359:** 863–875.

Mineyuki, Y. (1999). The preprophase band of microtubules: Its function as a cytokinetic apparatus in higher plants. Int. Rev. Cytol. **187:** 1–49.

Moffatt, B.A., McWhinnie, E.A., Agarwal, S.K., and Schaff, D.A. (1994). The adenine phosphoribosyltransferase-encoding gene of *Arabidopsis thaliana*. Gene **143:** 211–216.

Molinier, J., Ramos, C., Fritsch, O., and Hohn, B. (2004). CENTRIN2 modulates homologous recombination and nucleotide excision repair in Arabidopsis. Plant Cell **16:** 1633–1643.

Morsomme, P., Dambly, S., Maudoux, O., and Boutry, M. (1998). Single point mutations distributed in 10 soluble and membrane regions of the *Nicotiana plumbaginifolia* plasma membrane PMA2 H^+-ATPase activate the enzyme and modify the structure of the C-terminal region. J. Biol. Chem. **273:** 34837–34842.

Murata, T., Sonobe, S., Baskin, T.I., Hyodo, S., Hasezawa, S., Nagata, T., Horio, T., and Hasebe, M. (2005). Microtubule-dependent microtubule nucleation based on recruitment of gamma-tubulin in higher plants. Nat. Cell Biol. **7:** 961–968.

Nacry, P., Camilleri, C., Courtial, B., Caboche, M., and Bouchez, D.

(1998). Major chromosomal rearrangements induced by T-DNA transformation in Arabidopsis. Genetics **149:** 641–650.

Paredez, A.R., Somerville, C.R., and Ehrhardt, D.W. (2006). Visualization of cellulose synthase demonstrates functional association with microtubules. Science **312:** 1491–1495.

Pastuglia, M., Azimzadeh, J., Goussot, M., Camilleri, C., Belcram, K., Evrard, J.-L., Schmidt, A.-C., Guerche, P., and Bouchez, D. (2006). Gamma-tubulin is essential for microtubule organization and development in *Arabidopsis.* Plant Cell **18:** 1412–1425.

Pastuglia, M., and Bouchez, D. (2007). Molecular encounters at microtubule ends in the plant cell cortex. Curr. Opin. Plant Biol. **10:** 557–563.

Popovici, C., Zhang, B., Gregoire, M.J., Jonveaux, P., Lafage-Pochitaloff, M., Birnbaum, D., and Pebusque, M.J. (1999). The t (6;8)(q27;p11) translocation in a stem cell myeloproliferative disorder fuses a novel gene, FOP, to fibroblast growth factor receptor 1. Blood **93:** 1381–1389.

Rieder, C.L., Faruki, S., and Khodjakov, A. (2001). The centrosome in vertebrates: More than a microtubule-organizing center. Trends Cell Biol. **11:** 413–419.

Romio, L., Wright, V., Price, K., Winyard, P.J., Donnai, D., Porteous, M.E., Franco, B., Giorgio, G., Malcolm, S., Woolf, A.S., and Feather, S.A. (2003). OFD1, the gene mutated in oral-facial-digital syndrome type 1, is expressed in the metanephros and in human embryonic renal mesenchymal cells. J. Am. Soc. Nephrol. **14:** 680–689.

Salisbury, J.L. (1995). Centrin, centrosomes, and mitotic spindle poles. Curr. Opin. Cell Biol. **7:** 39–45.

Salisbury, J.L., Suino, K.M., Busby, R., and Springett, M. (2002). Centrin-2 is required for centriole duplication in mammalian cells. Curr. Biol. **12:** 1287–1292.

Santoni, V. (2007). Plant plasma membrane protein extraction and solubilization for proteomic analysis. Methods Mol. Biol. **355:** 93–109.

Schlaitz, A.L., et al. (2007). The *C. elegans* RSA complex localizes protein phosphatase 2A to centrosomes and regulates mitotic spindle assembly. Cell **128:** 115–127.

Schwarz-Sommer, Z., Hue, I., Huijser, P., Flor, P.J., Hansen, R., Tetens, F., Lonnig, W.E., Saedler, H., and Sommer, H. (1992). Characterization of the Antirrhinum floral homeotic MADS-box gene deficiens: Evidence for DNA binding and autoregulation of its persistent expression throughout flower development. EMBO J. **11:** 251–263.

Shaw, S.L., Kamyar, R., and Ehrhardt, D.W. (2003). Sustained microtubule treadmilling in Arabidopsis cortical arrays. Science **300:** 1715–1718.

Stoppin, V., Vantard, M., Schmit, A.C., and Lambert, A.M. (1994). Isolated plant nuclei nucleate microtubule assembly: The nuclear surface in higher plants has centrosome-like activity. Plant Cell **6:** 1099–1106.

Stoppin-Mellet, V., Canaday, J., and Lambert, A.M. (1999). Characterization of microsome-associated tobacco BY-2 centrins. Eur. J. Cell Biol. **78:** 842–848.

Sugiyama, N., Nakagami, H., Mochida, K., Daudi, A., Tomita, M., Shirasu, K., and Ishihama, Y. (2008). Large-scale phosphorylation mapping reveals the extent of tyrosine phosphorylation in Arabidopsis. Mol Syst Biol **4:** 193.

Thompson, J.D., Higgins, D.G., and Gibson, T.J. (1994). CLUSTAL W: Improving the sensitivity of progressive multiple sequence alignment through sequence weighting, position-specific gap penalties and weight matrix choice. Nucleic Acids Res. **22:** 4673–4680.

Traas, J., Bellini, C., Nacry, P., Kronenberger, J., Bouchez, D., and Caboche, M. (1995). Normal differentiation patterns in plants lacking microtubular preprophase bands. Nature **375:** 676–677.

Van Damme, D., Coutuer, S., De Rycke, R., Bouget, F.Y., Inze, D., and Geelen, D. (2006). Somatic cytokinesis and pollen maturation in Arabidopsis depend on TPLATE, which has domains similar to coat proteins. Plant Cell **18:** 3502–3518.

Van Damme, D., Vanstraelen, M., and Geelen, D. (2007). Cortical division zone establishment in plant cells. Trends Plant Sci. **12:** 458–464.

Van Leene, J., et al. (2007). A tandem affinity purification-based technology platform to study the cell cycle interactome in *Arabidopsis thaliana*. Mol. Cell. Proteomics **6:** 1226–1238.

Voinnet, O., Rivas, S., Mestre, P., and Baulcombe, D. (2003). An enhanced transient expression system in plants based on suppression of gene silencing by the p19 protein of tomato bushy stunt virus. Plant J. **33:** 949–956.

Walker, K.L., Muller, S., Moss, D., Ehrhardt, D.W., and Smith, L.G. (2007). Arabidopsis TANGLED identifies the division plane throughout mitosis and cytokinesis. Curr. Biol. **17:** 1827–1836.

Wasteneys, G.O. (2002). Microtubule organization in the green kingdom: Chaos or self-order? J. Cell Sci. **115:** 1345–1354.

Weingartner, M., Binarova, P., Drykova, D., Schweighofer, A., David, J.P., Heberle-Bors, E., Doonan, J., and Bogre, L. (2001). Dynamic recruitment of Cdc2 to specific microtubule structures during mitosis. Plant Cell **13:** 1929–1943.

Yan, X., Habedanck, R., and Nigg, E.A. (2006). A complex of two centrosomal proteins, CAP350 and FOP, cooperates with EB1 in microtubule anchoring. Mol. Biol. Cell **17:** 634–644.

Zimmermann, P., Hirsch-Hoffmann, M., Hennig, L., and Gruissem, W. (2004). GENEVESTIGATOR. Arabidopsis microarray database and analysis toolbox. Plant Physiol. **136:** 2621–2632.